SEMIANNUAL STATUS REPORT

For the Period

November 21, 1974 through May 20, 1975

NASA NSG 3008

ACCIDENTAL NON-IDEAL EXPLOSIONS

Dr. Robert Siewert, Technical Monitor

by

Roger A. Strehlow

Aeronautical and Astronautical Engineering Department
University of Illinois
June 10, 1975

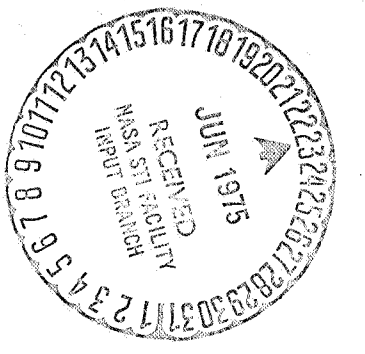

During the past 6 months we have made progress in the following areas of research:

1. Comprehensive survey of the literature for all types of explosions.
2. Study blast wave behavior from simple pressure vessel bursts.
3. Energy addition studies.
4. Study energy distribution between source volume and surroundings for different explosion processes.
5. Back calculation studies.

Current status and future plans for each of these areas of study will be discussed in the next five sections of this report.

SURVEY OF THE LITERATURE

This survey is complete. It is being forwarded to NASA Lewis Laboratories for printing as a NASA CR report and distribution.

SIMPLE PRESSURE VESSEL BURST

This study is reasonably complete. It was discovered during the analysis of 10 numerical calculations with different initial conditions that a single overpressure versus scaled distance nomograph for all spherical pressure vessel bursts could be constructed from the computer output. The initial point on the nomograph can be determined easily if the pressure, velocity of sound and heat capacity ratio of the gas in the vessel are known. These are the pertinent variables according to Baker's analysis as presented in the last status report. At present we are not sure how positive impulse will scale and we do not have sufficient data reduced to allow a clean cut decision to be made on this point. We should complete both the overpressure and positive impulse modeling during the next 6 months. The results of this work have yielded a thesis for Mr. Ricker and are being written up for presentation at the Fifth International Symposium on Explosions and Reactive Systems to be held in Bourges, France, in September.

SwRI is planning to start experimenting with bursting glass spheres to learn how the blast wave in the near field is modified by the presence of fragments.

ENERGY OF ADDITION STUDIES

We have approximately 23 computer runs in which energy was added slowly to a central region of the flow. The basic grid contains nine cases.

The central point on the grid is a control point and calculations were also made for an increase and decrease by an order of magnitude in both the energy and the rate of energy addition, yielding 8 additional basic calculations. The energy addition was exponential in time with a time for addition of 0.2 t_o at the central point where t_o is the time it takes a sound signal to travel from the edge of the ball to the center. The energy was added homogeneously to the gas inside the ball volume. The other runs were made to check on the effects of varying a number of important parameters. In each case only one parameter was varied at a time. For example, net size was changed to check reproducibility, energy was added as a cosine function in time, as a cosine function in space, as a double ramp function, etc., etc.

The results of these runs are currently being analyzed in detail. They will yield a Ph.D. thesis for Mr. Adamczyk and will thereafter be written up for the open literature.

ENERGY DISTRIBUTION AT LATE TIME

A paper is in preparation in which we examine the energy distribution, at late time, between the source volume and the surroundings. This is calculated by estimating the p,v behavior of the contact surface during the explosion process to determine the quantity of energy which is eventually deposited in the surroundings. Six distinct energy addition processes have been studied. These are: I. Constant pressure energy addition. II. Constant volume energy addition followed by isentropic expansion against an always equal counterpressure. III. The bursting sphere. IV. Constant velocity piston with finite stroke. V. Constant velocity flame with finite flame ball size, and VI. Spherical CJ detonation.

It was found that the quantity E_S/Q, which represents the relative quantity of energy transfered to the surroundings varied from $(\gamma_1-1)/\gamma_1$ to 1 depending on the process involved (here γ_1 is the heat capacity ratio of the working fluid in the ball) and that for the $(\gamma_1-1)/\gamma_1$ limit no blast is transmitted to the surroundings while for the 1 limit, point source behavior is obtained.

These results lead us to question the concept of far field equivalency as applied to all explosions. In regard to this work we have also discovered a simple way to replace the ΔH_c of a hydrocarbon by a more useful variable to represent energy addition due to combustion, whether it be detonation, flame propagation or constant volume or constant pressure combustion. It turns out that the actual Hugoniot of the combustion products can be easily curve fitted to the rectangular hyperbola which represents heat addition to a constant gamma gas. This curve fit yields a value of Q and γ which can now be used in conjunction with the E_S/Q results developed in the earlier part of this phase of the work. This work is being written up as a paper for submission to Combustion and Flame.

BACK CALCULATION TECHNIQUE

This technique has been developed and compared to a forward calculation for one case with reasonably good agreement. A detailed description of the technique, written by Dr. Frank Dodge, is included as Appendix A. The technique will next be applied to some real records which have been obtained from Mrs. Hyla Napadensky at IIT Research Institute, Chicago, Ill. We now realize that the technique will only calculate E_S, the energy imparted to the surroundings by the explosion. However, this technique in conjunction with the E_S/Q theory discussed in the previous section should

yield a reasonable estimation of Q for any accidental explosion that can be evaluated by back calculation.

BIBLIOGRAPHY

The following reports are either completed or in preparation in connection with this grant.

1. The Characterization and Evaluation of Accidental Explosions by Roger A. Strehlow and Wilfred E. Baker. NASA CR 134779. June 1975

2. Blast Waves from Bursting Pressurized Spheres. Randall E. Ricker, M.S. Thesis, University of Illinois (1975). To be written as a paper for presentation at Bourges, France, September 1975.

3. Terminal Energy Distribution for Non-Ideal Blast Waves. R. A. Strehlow and A. A. Adamczyk. Combustion and Flame - to be submitted soon.

4. A Study of Blast-Waves Generated by Non-Ideal Energy Sources by A. A. Adamczyk, Ph.D. Thesis, in preparation.

APPENDIX A

DETERMINATION OF ENERGY-RELEASE FUNCTION

by Dr. Frank Dodge
Southwest Research Institute

1. Introduction

There is not yet a general theoretical model that makes it possible to unify all the diverse data available from non-ideal explosions, partly because of the great difficulty in measuring the energy released by the explosive reaction. In most experiments only the blast wave characteristics are or can be measured, which makes it necessary to determine the energy released by some other method. Strehlow, Savage, and Vance (Ref. 1) have outlined a method of back-calculating the explosive energy released that uses only experimental pressure data, which if verified might provide the needed link between experimental data and the development of a general theoretical model. The objective of this task was, in fact, to devise a computer code along the lines sketched in Ref. 1 and to determine if the proposed method of computing the energy released was valid. There were some questions about whether the assumptions made in Ref. 1 that connected the flow field to the energy released by the explosion were not overly idealized, but because of the overall progress made in the various tasks of this program, more realistic assumptions are now possible. In addition, the procedure outlined in Ref. 1 was limited to experimental data that contained no shock waves; a tentative method of incorporating shocks is outlined herein, although these kinds of calculations have not been included in the present results.

In brief, the method outlined in Ref. 1 uses pressure vs. time

data at a fixed spatial location as starting conditions for a technique based on the method of characteristics. The entire flow field is calculated backward in time and space until the cloud of explosive gases is reached. Inferences are made about the energy contained in the cloud, using some thermodynamics- and chemistry-based assumptions. The partitioning of this energy between the flow field and the explosive gases are obtained by using the computed details of the flow field. This procedure therefore allows the energy released by the explosion to be correlated with the over-pressures that are generated (i.e., destructiveness), the far-field equivalence to TNT, etc.

2. Starting Conditions for Calculations

A typical experimental set-up is sketched in Figure 1. The pressure gage located at the radial distance R_G from the site of the explosion records the pressure as a function of time. This record, the distance R_G, and the time $t = 0$ at which the explosion begins are presumably all the data available.

In order to start the back-calculations of the flow field, two of the flow variables must be known for all time $t > 0$ at $R = R_G$. (This implies, incidentally, that arbitrary assumptions about the pressure and, say the particle velocity at $T = R_G$ are not possible, and that the relation between the pressure and the velocity must be a solution of the equations of motion.) The experimental pressure data provide one of the needed inputs, but the second must itself either be measured (which, if it is the particle velocity is not easily done and in any case not generally available) or derived solely from the pressure record, which is the method used here. Since the explosion is unconfined, the flow contains only a simple

wave emanating from a simple source. With this kind of wave system, there is a unique relation between the pressure vs. time curve at $R = R_G$ and the particle vs. time curve, as contrasted to a wave system including reflected waves for which the particle velocity can not be computed solely from a pressure record.

When the maximum pressure is not too much larger than ambient, the velocity can be calculated by acoustic methods (Refs. 2 and 3). For acoustic waves, the particle velocity u at $R = R_G$ is:

$$u(R_G,t) = \frac{a_o^2}{R_G} \int_o^t s \cdot dt + a_o s \tag{1}$$

In Eq. (1), a_o is the ambient speed of sound and $s = (\rho - \rho_o)/\rho_o$ is the "condensation," where ρ is the density of the air in the wave system and ρ_o is the ambient density. For an ideal gas, the condensation can be related to the pressure p by:

$$s = \left(\frac{p}{p_o}\right)^\gamma - 1 \simeq \frac{\Delta p}{\gamma p_o} \quad (\Delta p = p - p_o) \tag{2}$$

where the last approximation follows from the assumed smallness of the over-pressure. Eqs. (1) and (2) allow the velocity at $R = R_G$ to be calculated solely from a pressure record, for acoustic waves.

Ref. (1) gives a modification of Eq. (1) to allow larger over-pressures, using a first order correction term to the velocity of sound, a. For an ideal gas $a^2 = \gamma p/\rho$, so to the first approximation:

$$a = a_o[1 + \tfrac{1}{2}(\gamma-1)s] \tag{3}$$

The particle velocity is therefore:

$$u(R_G,t) = \frac{a_0}{R_G}[1+(\gamma-1)s] \int_o^t s \cdot dt + a_o[1 + \tfrac{1}{2}(\gamma-1)s]s \tag{4}$$

A further refinement can be made by applying acoustic theory locally, i.e., by superimposing an acoustic "wavelet" on a wave of finite amplitude (Ref. 4.). This approximation gives

$$u(R_G,t) = \frac{a_o^2}{R_G} \int_o^t \frac{1}{\gamma} \left(\frac{p}{p_o}\right)^{\frac{\gamma-1}{\gamma}} \ln \frac{p}{p_o} \cdot dt + \frac{2a_o}{\gamma-1}\left[\left(\frac{p}{p_o}\right)^{\frac{\gamma-1}{2\gamma}} - 1\right] \qquad (5)$$

In any of the methods, the integration with respect to time must be performed numerically.

As mentioned previously, the pressure and velocity at $R = R_G$ must be a solution of the equations of motion. The accuracy of the various approximations, Eqs. (1), (4), or (5), can only be checked, therefore, by experimental data for both pressure and velocity or by numerical results from available computer codes for simplified forms of non-ideal explosions. Since experimental data are not currently available, numerical data were used here. These solutions, which were provided by A. A. Adamczyk, were computed for the very rapid addition of heat to a spherical cloud of ideal gas (Ref. 5). A typical pressure pulse in the surroundings at a distance R_G equal to three times the initial cloud radius R_o, is shown in Figure 2. This pulse is characterized by a strong compression wave that passes the pressure gage location at a non-dimensional time of about 2.9 (which corresponds to an actual time of $2.9 \times \sqrt{1.4} = 3.4$ times the time required for a sound wave to travel outward from the center of the cloud to its original boundary, when the gas is at its initial temperature). The velocity induced by this system of out-going waves is shown in Figure 3, as are sample results calculated by inserting the pressure data of Figure 2 into Eqs. (1), (4), and (5). All of the approximations reproduce the general shape of the velocity vs. time record, but the wavelet approximation, Eq. (5), has the

smallest maximum error. (The error at a given time is the discrepancy in velocity divided by the maximum velocity, $u = 0.312\theta_o$). The wavelet method is therefore used hereafter to calculate starting velocities.

The wavelet approximation probably is accurate enough to calculate reasonable starting velocities even for much stronger compressions waves, as is discussed in Section 5.

3. Back-Calculations by Method of Characteristics

The method of characteristics (that is, projecting characteristics from points where the flow variables are known to points where the flow variables are desired) is a common solution technique for one-dimensional, unsteady, compressible flow (Ref. 6). In its pure form, however, it is extremely unwieldy for use in computer solutions, and the Hartree or "constant time step" modification is the most common method of application for computing the flow that result from any specified disturbance (Ref. 7). Figure 4a shows how the Hartree scheme would be applied to a system of simple, outgoing waves, which will be discussed briefly to contrast it with the scheme developed here. The disturbance can be specified along any line in the distance vs. time space that is not a characteristic of the flow. Two of the flow variables must be specified along an initial data line t = constant, but there is no interrelationship between the pressure and the velocity along this line that must be satisfied. The flow variables for a time advanced everywhere by Δt are calculated from the known disturbance and the flow information carried forward with the characteristics. A point on the advanced time line (say, point 4) is located approximately by projecting forward the particle path (i.e., a line with the slope $dR/dt = 1/u_2$) from a point 2 on the intial data line.

The "P" and "Q" characteristics (lines with slope $1/(u + a)$ and $1/(u-a)$ respectively) are then dropped back until they intersect the initial data line, simultaneously interpolating between 1 and 2, and 2 and 3, to determine the required flow variables for these characteristics. The flow information carried forward along the characteristics to 4 is used to calculate the flow variables at 4, after which all the slopes are corrected and iterative calculations are performed until convergence is satisfied. The conditions for numerical stability have been shown to be that $\Delta t < R/a$ over the entire initial data line. Otherwise the flow variables at 4 are influenced by data lying outside the characteristics through 1 and 3.

It is clear that the Hartree method is not applicable to the problem of back-calculating the flow generated by a system of outgoing waves. For this, the pressure and velocity at a fixed location $R = R_G$ for all $t > 0$, as well as the pressure ($p = p_o$) and velocity ($u = 0$) along the line $t = 0$ lying to the right of the source of the waves (i.e., the cloud of gases), are the known conditions, and the disturbance that caused the flow is sought. A new "constant distance step" technique has therefore been devised, as sketched in Figure 4b. Although at first glance the constant time step and the constant distance step procedures seem analogous, there are several important differences. The particle path through the new point (say, point 4) will not lie without the area formed by the characteristics intersecting at 4, except for a supersonic flow, and since the point of originiation of this particle path will not be known even approximately in advance of calculating the flow variables at 4, there is no need to project the particle paths for this method. Instead the "Q" characteristic through one of the points on the initial data line (say, point 1) is

projected backward to locate 4 approximately. From 4, a "P" characteristic is projected forward to locate a point 3 on the initial data line, using interpolation between 1 and 2 to determine the slope of the characteristic. Iterating on the location of 4 and 3, using corrected values of the average slopes, velocities, etc., is repeated until the solution convergences. The flow properties of point 4 can be calculated, and so on. Details are given in the Subappendix.

The stability criterion relating ΔR to the chosen values of Δt can be explained with reference to Figure 5a and 5b. The distance step ΔR must be chosen small enough so that each of the new points lies inside the zone of influence of the two appropriate points on the initial data line. Otherwise, as the dashed lines indicate, the flow variables at the new point will be influenced by data not on the initial data line. For either subsonic or supersonic flow, it turns out that:

$$\Delta R < \frac{1}{2} a \cdot \Delta t \left| 1 - \frac{u^2}{a^2} \right| . \qquad (6)$$

When the flow is locally sonic ($u = a$) it appears that $\Delta R = 0$; that is, the calculations cannot progress. This corresponds to the coincidence of a characteristic and the data line, which if it occurs at other than isolated or singular points, causes the method of characteristics to break down; in other words, the problem is not well-posed (Refs. 8 and 9). It is unlikely in a system of outgoing waves generated by an explosion that the velocity will be sonic except at isolated instants of time along any line R = constant; therefore, the method of characteristics ought to be applicable here. (For the Hartree constant time step method, a characteristic and a data line can never coincide.) Figure 5c shows a case where the velocity increases from subsonic through sonic (at a discrete time) and

on into the supersonic range. As can be seen, the way the "P" and "Q" characteristics are projected backward to locate a new point changes from one side of the sonic point to the other, with the result that the entire new data line can be "filled in" completely without using the "Q" or vertical, characteristic through the sonic point. That is, there are no regions on the new line for which the flow variables can not be calculated, for any $\Delta t > 0$ on the initial line; each of the points on the new data line has "P" and "Q" characteristics which when projected forward lie within the data between the appropriate points on the initial line; and all the data points on the initial line are used in calculating the new data. This seems to indicate that the constant ΔR method is applicable even when the flow is sonic, if the sonic velocity occurs only at discrete points; if two adjacent points have $u = a$ (corresponding to sonic flow for a finite time), however, the entire method of characteristics is not applicable. During the current effort, only cases involving subsonic flow have been investigated, so numerical difficulties that might be encountered with sonic flow at discrete points have not been evaluated in practice.

A computer program has been written to implement the constant distance step procedure. Typical results for overpressure and particle velocity, compared to their "exact" values are shown in Figure 6. The starting conditions for these calculations were shown previously in Figure 2 and 3. (Only part of the calculated data is shown for clarity.) The back calculations compare reasonably well with the exact results. The major difference between the two is that the back-calculation method has tended to smooth the abrupt changes in the slope of the exact curves. There are several reasons for this. A value of Δt was used for the starting conditions that was just small enough to resolve the changes in slope in the

data for $R = R_G$, and this relatively large Δt created a fairly coarse computing mesh, thus tending to smooth the calculations. Also, the "exact" starting data are the results of numerical calculations and thus are not an exact solution of the equations of motion. In particular, the conservation of mass requirement in the original starting data (using the known "exact" velocity and not Eq. (5) was checked by finite difference calculations and found to contain a discrepancy of the order of 0.1%. This discrepancy propagates back through the calculations in the constant distance step method, and while the error does not increase without bound, this is another source of smoothing in the results. Taking these facts into account, the comparison displayed in Figure 6 is a satisfactory verification of the method and of the computer code.

4. Energy-Release Computations

The energy added to the surroundings by the explosion can be evaluated after the flow variables (pressure, temperature, velocity, etc.) have been calculated. There are several ways to make this evaluation.

With reference to Figure 7, the initial size of the effective cloud of explosive gases, at the instant the release of energy begins, is obtained by projecting the "P" characteristic backward from the point on the initial data line $R = R_G$ for which the pressure first rises above ambient, until it intersects the line $t = 0$. If there are no shock waves, the slope of this characteristic is constant and equal to $1/a_o$, so $R_o = R_G - a_o t_o$. (If a shock wave overtakes the initial wave, the slope of the characteristic changes, and this must be accounted for, as will be discussed in Section 5.) The particle path originating at $R = R_o$, $t = 0$, is traced out by using the already computed particle velocities; this path is the contact surface

separating the surroundings from the explosive cloud. The final size of the cloud, $R = R_f$, is calculated by projecting the "P" characteristic backward from the initial data line, at the instant the velocity equals zero and the pressure remains at ambient.

The energy added to the surroundings is equal to the kinetic energy that has flowed outward from the sphere $R = R_G$ plus the internal energy stored in the spherical shell $R_f \leq R \leq R_G$ at $t = t_f$. (There is no kinetic energy left in the shell $R_f \leq R \leq R_G$ after the wave system passes R_G.) Thus

$$E_s = 4\pi R_G^2 \int_{t_o}^{t_f} \rho V^3 \cdot dt + 4\pi C_V \int_{R_f}^{R_G} \rho(T-T_o)R^2 dR \qquad (7)$$

where C_V is the specific heat at constant volume. Alternatively, the energy added to the surroundings can be evaluated by considering the work done on it by the expanding cloud. Thus

$$E_s = 4\pi \int_{R_o}^{R_f} pR^2 \cdot dR \qquad (8)$$

where p is the pressure of the surroundings at the contact surface. (Equation (8) may be the most convenient to use for numerical calculations. This part of the computer program has not yet been completed, so the relative advantages of Eqs. (7) and (8) have not been tested.)

The energy transferred to the surroundings can be coupled to the total energy deposited in the cloud by the use of results derived by Strehlow and Adamczyk (Ref. 10).

5. Recommendations for Further Work

There are several sub-tasks that need to be completed in order to

make the computer code of maximum benefit. Clearly, the verification of the energy-release computations should be completed, as outlined in Section 4, by comparing the numerical predictions to both actual experiments where the explosive energy is known (e.g., bursting spheres) and to numerical solutions for cases of adding heat rapidly to a finite volume of gas (e.g., the examples discussed in Section 2).

It was pointed out in Section 3 that errors in the starting conditions, in the sense that the pressure and particle velocity used to begin the back calculations are not solutions of the equations of motion, are propagated throughout the flow field. This will be especially troublesome when actual experimental pressure records are the input. One way to diminish the possible errors is to make sure that the input satisfies conservation of mass. Starting with tentative data computed from Eq. (5), this can be done by determining the velocities and densities on the data line $R = R_G - \Delta R.$ and then using the velocities and densities for $R = R_G$ and $R = R_G - \Delta R$ to check conservation of mass by a finite difference technique. The velocities along the initial data line would be altered in an iterative manner, re-computing the velocities and densities along $R = R_G - \Delta R$ each time, until conservation of mass is satisfied. Figure 8 indicates one way to do this. Forward differences in time and backward differences in space are used. The density everywhere along the initial data line is known since $\rho = \rho_o(p/p_o)^{1/\gamma}$ (unless shock waves are present). Therefore, only the computed velocities for $R = R_G$ can be in error. In Figure 8, the velocity u_1' and density ρ_1' are interpolated from the computed points along the new data line. The velocity on $R = R_G$ is changed to make the finite difference form of the conservation mass equation identically equal to zero. (Changing u_1 will also eventually change u_1'

and ρ_1' but to a much smaller degree.) In this way, the velocities along $R = R_G$ can be altered one at a time to satisfy conservation of mass. Then, the velocities and densities along the new data line can be re-computed, and the process repeated until the calculations converge. Although this process is not without errors, because the kind of finite-difference grid used is known to be less accurate than centered differences, it should greatly improve the accuracy of the computed starting velocities.

Another desirable modification to the computer code is the capability to include shock waves. Significant numerical difficulties can arise when there is a shock in the flow field, and, in fact, the method of characteristics alone can not be used to back-calculate the entire flow field. The shock creates a "shadow," as illustrated in Figure 9, through which the characteristics (in this case, the "P" characteristics) cannot be followed. Nonetheless, the method of characteristics combined with a finite difference technique can be used to compute the flow variables in the shadowed zone, and thereby generate the information needed to predict the characteristics. (The method of characteristics alone is sufficient elsewhere in the flow field.)

Assuming that the velocity can be computed along the initial line R_G, the finite difference form of the conservation of mass equation (similar to Figure 8) can be used as an extra polation technique to give one equation relating ρ and u at, say, point C in Figure 9. The known value of the "Q" Riemann variable at point C gives a second independent relation between ρ and u. Therefore, ρ and u at C can be determined, and the corresponding "P" variable generated. A similar technique can be used to find the variable at C on the back side of the shock, and likewise points

elsewhere along the shock can be computed for each distance step. Since the flow variables can change rapidly in the vicinity of a shock, the finite difference gridwork needs to be relatively fine. Note that the finite difference method is not used to cross a shock; instead, the Rankine-Hugoniot relations are used to relate the flow variables on either side of the shock (Ref. 11).

The starting velocities cannot be determined directly from Eq. (5) when the pressure record contains a shock. For weak shocks (i.e., pressure ratios across the shock of 2.5 or less) the flow field can still be considered approximately isentropic (Ref. 6) so Eq. (5) can be used if the velocity jump across the shock Δu is computed separately by the Rankine-Hugoniot equations (Ref. 11); this is possible because the conditions on the upstream side of the shock are known. In the nomenclature of Figure 9, then, the starting velocities for weak shock waves are

$$u(R_G,t) = \frac{a_o^2}{\gamma R_G} \int_o^t \left(\frac{p}{p_o}\right)^{\frac{\gamma-1}{\gamma}} \ln \frac{p}{p_o} \cdot dt + \frac{2a_o}{\gamma-1}\left[\left(\frac{p}{p_o}\right)^{\frac{\gamma-1}{2\gamma}} -1\right], \quad t \le t_A \qquad (9)$$

and

$$u(R_G,t) = \Delta U_A + \frac{a_o^2}{\gamma R_G} \int_{t_A}^t \left(\frac{p}{p_o}\right)^{\frac{\gamma-1}{\gamma}} \ln \frac{p}{p_o} \cdot dt + \frac{2a_o}{\gamma-1}\left[\left(\frac{p}{p_o}\right)^{\frac{\gamma-1}{2\gamma}} -1\right], \quad t > t_A \qquad (10)$$

In Eq. (16), ΔU_A is computed from the Rankine-Hugoniot equations, using P_A and U_A as computed from Eq. (9) for $t = t_A$, as the upstream conditions.

For strong shocks, the starting conditions become more difficult to determine because each fluid particle passing through the shock has a change of entropy. If the shock is of constant strength, or nearly so, however, Eqs. (9) and (10) still apply because the change in entropy is a constant

for each particle. The flow field on either side of the shock is isentropic, and all the entropy change is taken up in ΔU_A. When the shock strength varies, as it would in most explosion-generated flow fields, the particles experience different entropy changes, and Eq. (10), which is derived for an isentropic flow, becomes increasingly more inaccurate. There is not an unimpeachable way, in fact, of determining the starting velocities for $t > t_A$ except by considering the known pressure distribution along $R = R_G$ as an initial distubance to the volume of space $R > R_G$, and then using the Hartree constant time method or equivalent to compute the flow field for $R = R_G$. This procedure would give the velocities along $R = R_G$, but it seems unduly complicated, at least until the computed code for non-strong shocks has been verified. It is therefore recommended that Eqs. (9) and (10) be used initially even for strong shocks.

6. Conclusions

A verified computer code, based on the method of characteristics, has been developed which uses as its only input the pressure pulse recorded by a gauge at some distance from a non-ideal explosion to compute the entire transient flow field (behind the gauge location) generated by the explosion. A method has been indicated to use these calculations to determine the energy released by the explosion. The energy-release formulation must be included in the code and verified. The indicated method for incorporating shocks should also be implemented.

It is believed that the insight provided by the results of this code, particularly the energy-release computations, will significantly aid the development of a general theoretical model of non-ideal explosions.

SUBAPPENDIX. Calculation of Flow Variables on New Data Line

The method will be outlined for a general point. Only the subsonic flow is discussed, but the same procedure holds for supersonic flow.

As a first guess, the position of point 4 (Figure A-1) on the new line is estimated by projecting the "Q" characteristic backward from point 1 as a straight line:

$$t_4 = t_1 - \left(\frac{1}{u_1-a_1}\right)\Delta R \tag{A-1}$$

The first guess of the position of the point 3, whose "P" characteristic crosses point 4 is estimated by projecting the "P" characteristic backward from point 3, using linear interpolation between 1 and 4 to determine simultaneously the properties at 3:

$$t_3 = t_1 + \left[\left[\left[U_1+a_1+\Delta R\left(\frac{u_2+a_2}{u_1-a_1}-1\right)\right]/(t_2-t_1)\right]^2 + 4\Delta R(u_1-a_1)\ x\right.$$

$$x\left(\frac{u_2+a_2}{u_1-a_1}-1\right)\left(1-\frac{u_1+a_1}{u_1-a_1}\right)/(t_2-t_1)\Bigg]^{1/2} - [u_1+a_1+$$

$$\left.+\Delta R\left(\frac{u_2+a_2}{u_1-a_1}-1\right)(t_2-t_1)\right]\Bigg]\Bigg/\left[2(u_1-a_1)\left(\frac{u_2+a_2}{u_1-a_1}-1\right)/(t_2-t_1)\right] \tag{A-2}$$

The first guess for the properties at 3 are thus

$$u_3 = u_1 + \left(\frac{t_3-t_1}{t_2-t_1}\right)(u_2-u_1) \tag{A-3}$$

$$a_3 = a_1 + \left(\frac{t_3-t_1}{t_2-t_1}\right)(a_2-a_1) \tag{A-4}$$

The Riemann variables $P = \left(\frac{2}{\gamma-1}\right)a + u$ and $Q = \left(\frac{2}{\gamma-1}\right) a - u$

at the new point 4 are:

$$P_4 = P_3 + \frac{2u_3a_3}{R-\frac{1}{2}\Delta R}(t_3-t_4) \tag{A-5}$$

$$Q_4 = Q_1 + \frac{2u_1a_1}{R-\frac{1}{2}\Delta R}(t_4-t_1) \tag{A-6}$$

Finally, the first guess for the velocity and speed of sound at 4 is:

$$U_4 = \frac{P_4-Q_4}{2} \qquad a_4 = \frac{(P_4+Q_4)(\gamma-1)}{4} \tag{A-7}$$

Now, an iteration process is begun to determine point 4 accurately, since the "P" and "Q" characteristics do not in fact have a constant slope. The average slope of the "Q" characteristic between 1 and 4 is $\tan[(\theta_1+\theta_{4_Q})/2]$ for example. Thus, the next guess for point 4 is:

$$t_4 = t_1 + \Delta R \tan[(\theta_1+\theta_{4_Q})/2] \tag{A-8}$$

where $\theta_1 = \arctan[1/(a_1-u_1)]$, $\theta_2 = \arctan[1/(a_4-u_4)]$, and either non-dimensional variables are used or it is understood that the tangents have dimensions of reciprocal velocity. The flow properties used in evaluating θ_{4_Q} are those corresponding to the previous iteration. Likewise,

$$t_3 = t_4 + \Delta R \tan[(\theta_3 + \theta_{4_P}/2] \tag{A-9}$$

where t_4 comes from Eq. (A-8), $\theta_3 = \arctan[1/(a_3+u_3)]$, $\theta_{4_P} = \arctan[1/(a_4+u_4)]$, and the flow properties used in evaluating θ_3 and θ_{4_P} correspond to the previous iteration. The new values of the flow properties at point 3 are computed from Eqs. (A-3) and (A-4). The flow variables at

point 4 are computed by:

$$P_4 = P_3 + \frac{(u_3 a_3 + u_4 a_4)}{(R - \frac{1}{2}\Delta R)} (t_3 - t_4) \qquad \text{(A-10)}$$

$$Q_4 = Q_1 + \frac{(u_1 a_1 + u_4 a_4)}{(R - \frac{1}{2}\Delta R)} (t_4 - t_1) \qquad \text{(A-11)}$$

Equations (A-7) are used to calculate the new u_4 and a_4. It has been found that convergence is accelerated by iterating upon Eqs. (A-7), (A-10) and (A-11) until u_4 and a_4 do not change.

New values of t_4 and t_3 are next calculated, and so on, until the locations of points 4 and 3 have been determined accurately.

The initial data point t_0 on the new line (i.e., the point where $u = 0$ and the pressure just starts to increase) is found from the equation

$$(t_0)_{new} = (t_0)_{old} - \Delta R/a_0 \qquad \text{(A-12)}$$

After the new line is filled in, the data is spread evenly by interpolation to give a constant ΔR between the points. Otherwise, it is found that a smaller than average Δt grows continually smaller, with the result that the allowable ΔR becomes smaller as the calculations progress.

REFERENCES

1. Strehlow, R. A., Savage, L. D., and Vance, Gary M., "On the Measurement of Energy Release Rates in Vapor Cloud Explosions," Combustion Science and Technology, 6, pp 307-312, 1973.

2. Lamb, H., Hydrodynamics, pp 489-495, Dover Publications, 1956.

3. Rayleigh, J. W. S., The Theory of Sound, Vol. II, pp 16, 109-114, Dover Publications, 1958.

4. Liepmann, H. W., and Roshko, A., Elements of Gasdynamics, pp 74-76, John Wiley and Sons, 1957.

5. Strehlow, R. A., and Adamczyk, A. A., "On the Nature of Non-Ideal Blast Waves," Tech. Rept. AAE 74-2, Grant AFOSR-73-2524, University of Illinois, April 1974.

6. Rudinger, G., Wave Diagrams for Nonsteady Flow in Ducts, D. van Nostrand, 1955.

7. Chou, P. C., Karpp, R. R., and Huany, S. L., "Numerical Calculation of Blast Waves by the Method of Characteristics," AIAA J., 5, pp 618-723, 1967.

8. Courant, R., and Friedrichs, K. O., Supersonic Flow and Shock Waves, Chapter II, Interscience, 1948.

9. Shapiro, A. H., The Dynamics and Thermodynamics of Compressible Fluid Flow, Vol. I, Appendix A, Ronald Press, 1953.

10. Strehlow, R. A., and Adamczyk, A. A., Terminal Energy Distribution for Non-Ideal Blast Waves. To be submitted to Combustion and Flame.

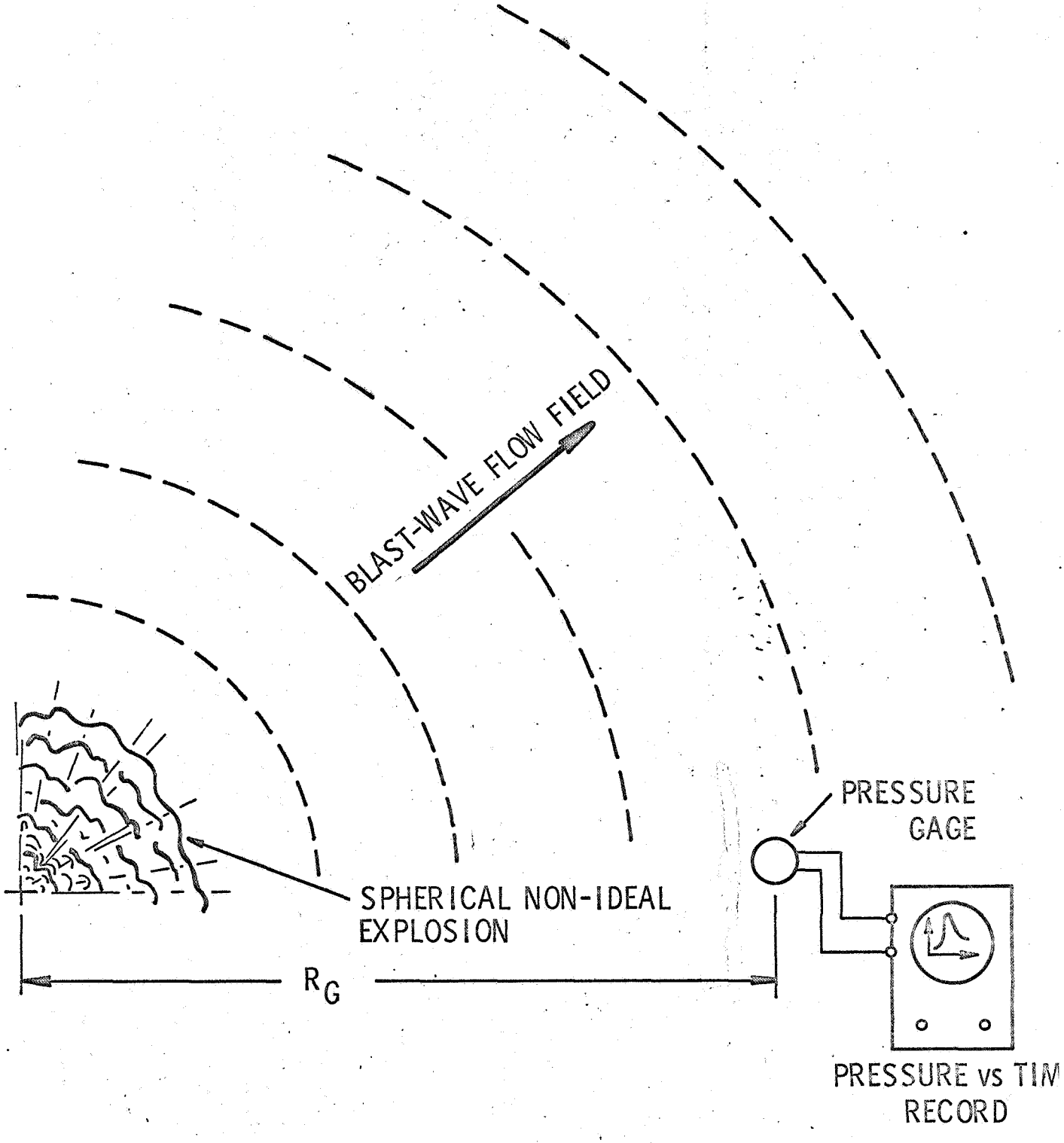

Figure 1. Model for Analysis of Non-Ideal Explosive Flow Field

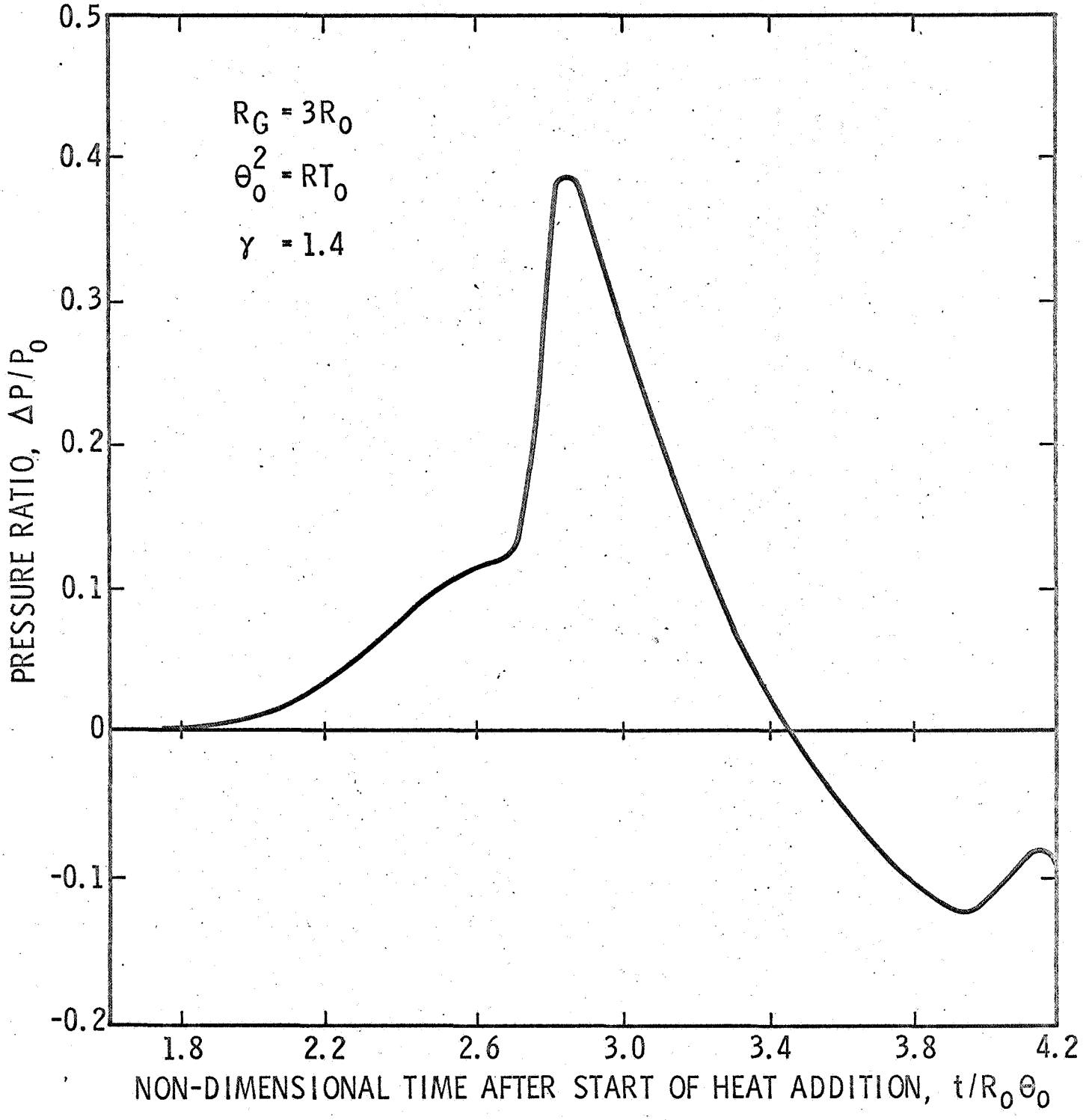

Figure 2. Pressure vs Time at $R_G = 3R_0$ for Sample Problem

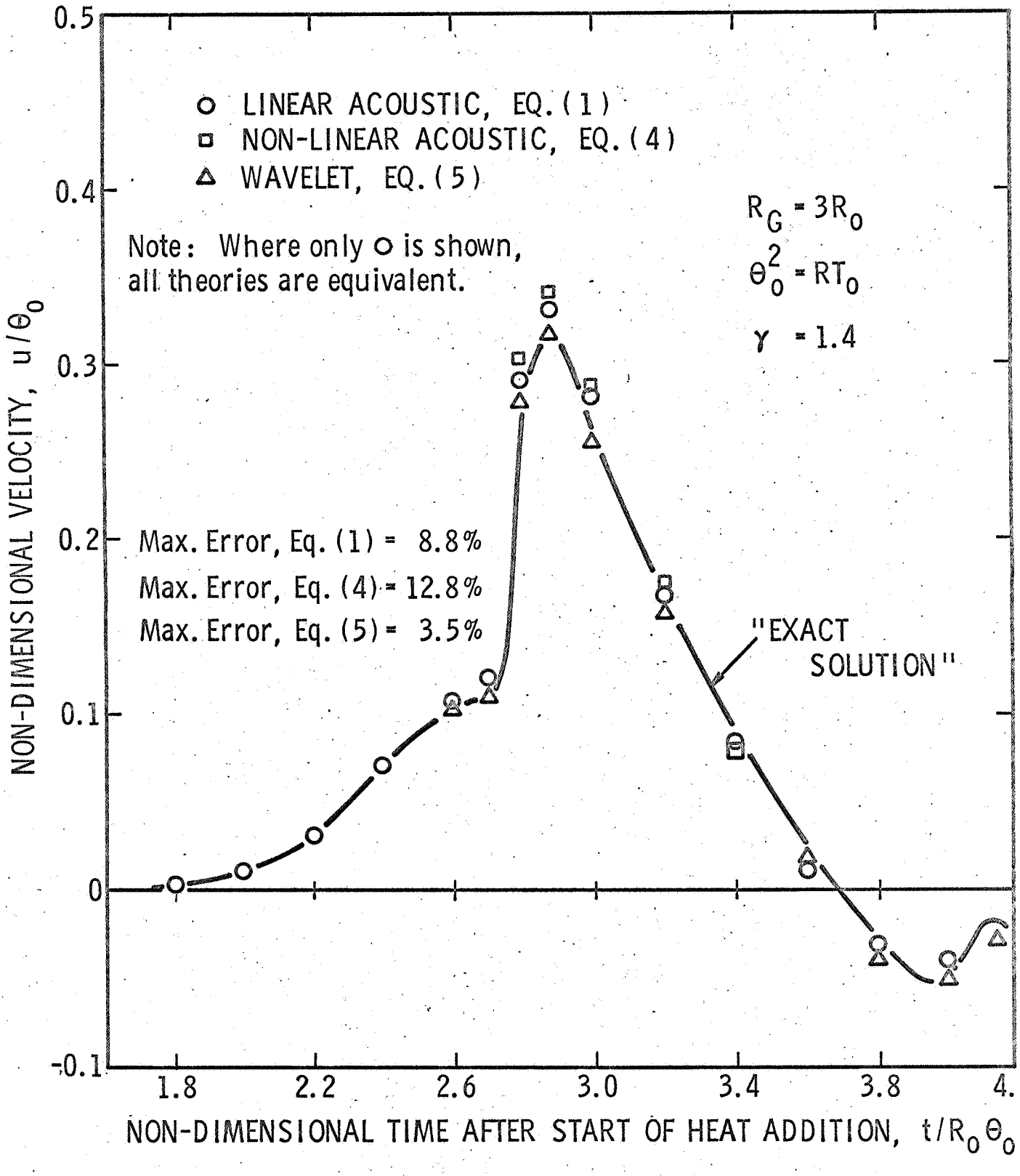

Figure 3. Comparison of Particle Velocities at $R_G = 3R_0$ for Sample Problem

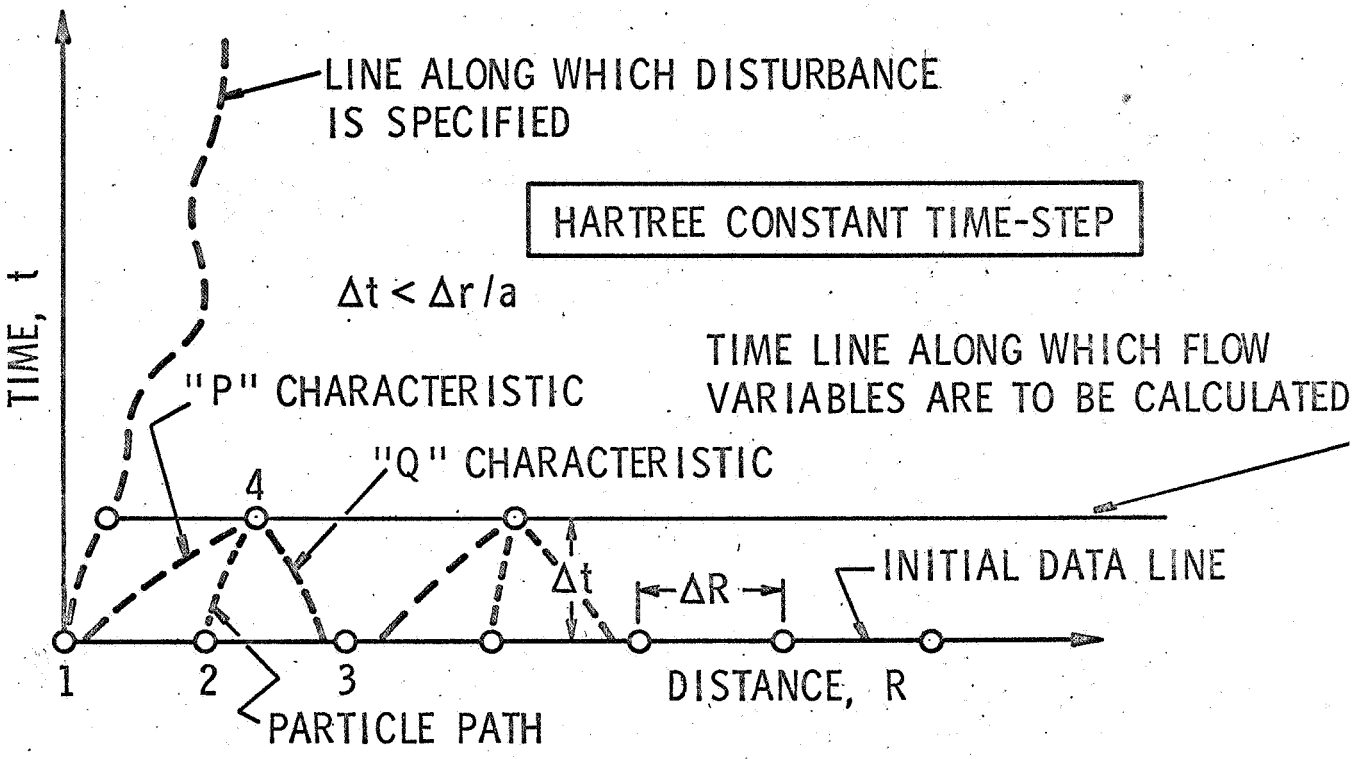

(a) Calculations carried forward in time

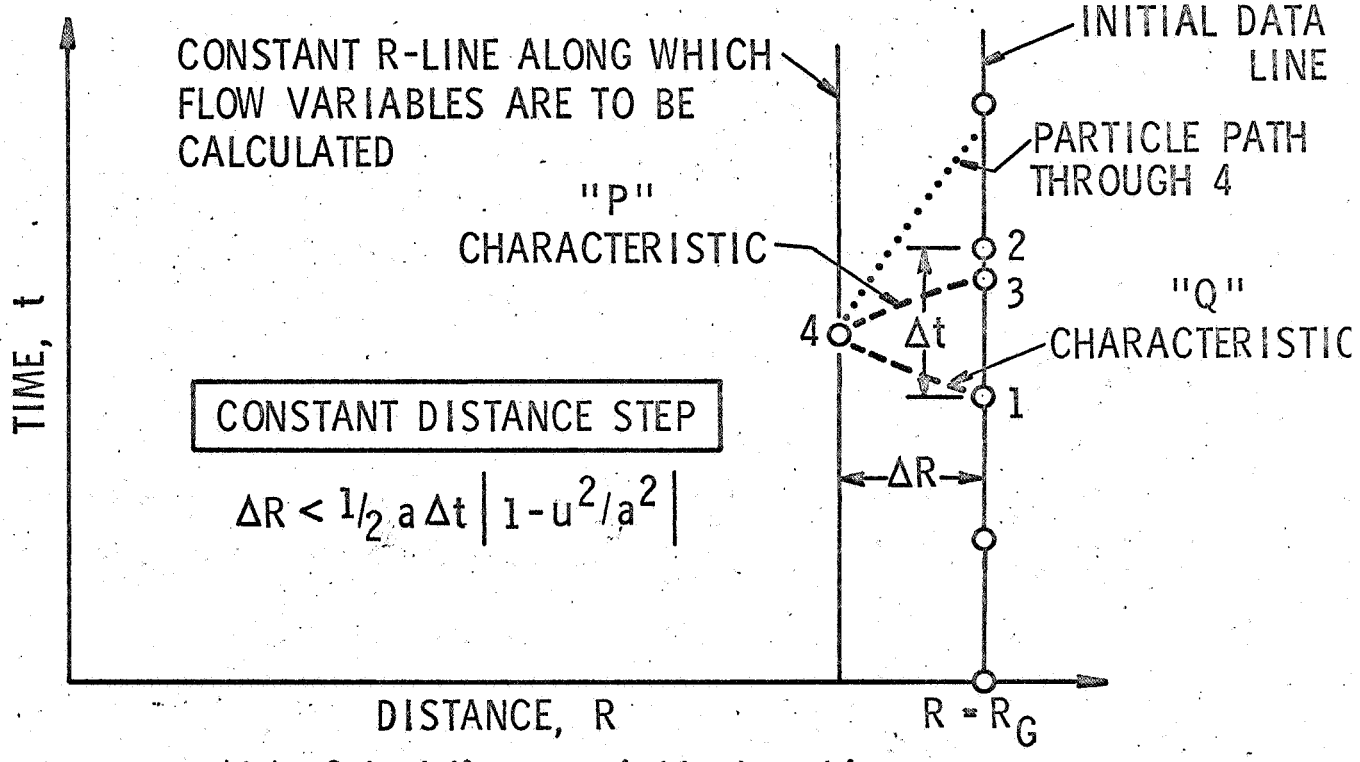

(b) Calculations carried backward in space

Figure 4. Method of Characteristics Models

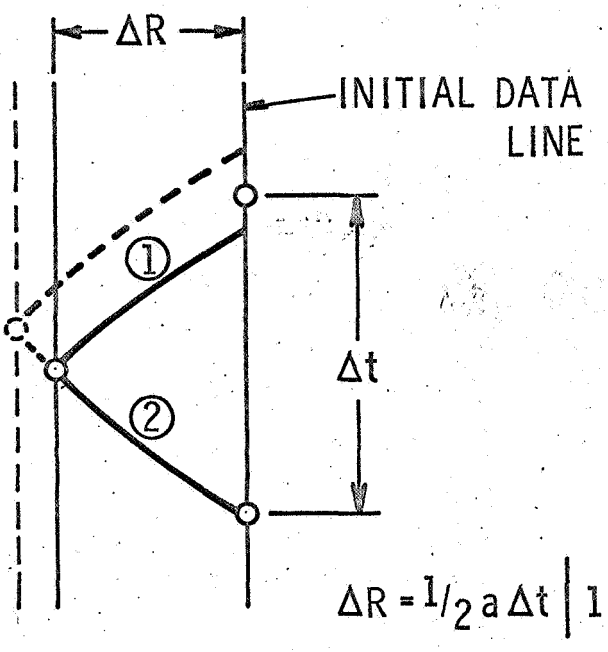

$$\Delta R = {}^1/_2\, a\, \Delta t \left| 1 - u^2/a^2 \right|$$

(a) Subsonic flow

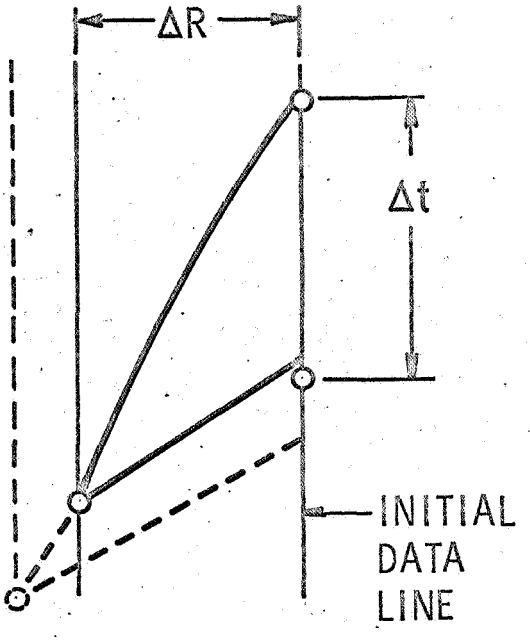

(b) Supersonic flow

① = "P" CHARATERISTIC,

$$\text{SLOPE} = \frac{dR}{dt} = \frac{1}{u + a}$$

② = "Q" CHARACTERISTIC,

$$\text{SLOPE} = \frac{dR}{dt} = \frac{1}{u - a}$$

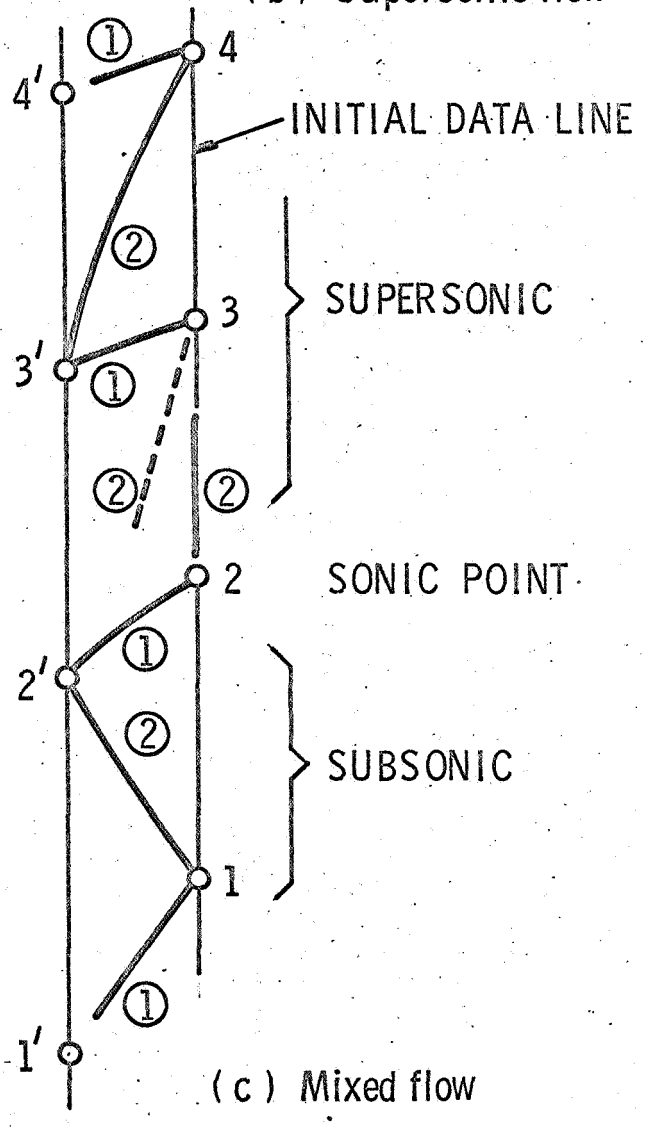

(c) Mixed flow

Figure 5. Stability Criteria for Constant ΔP

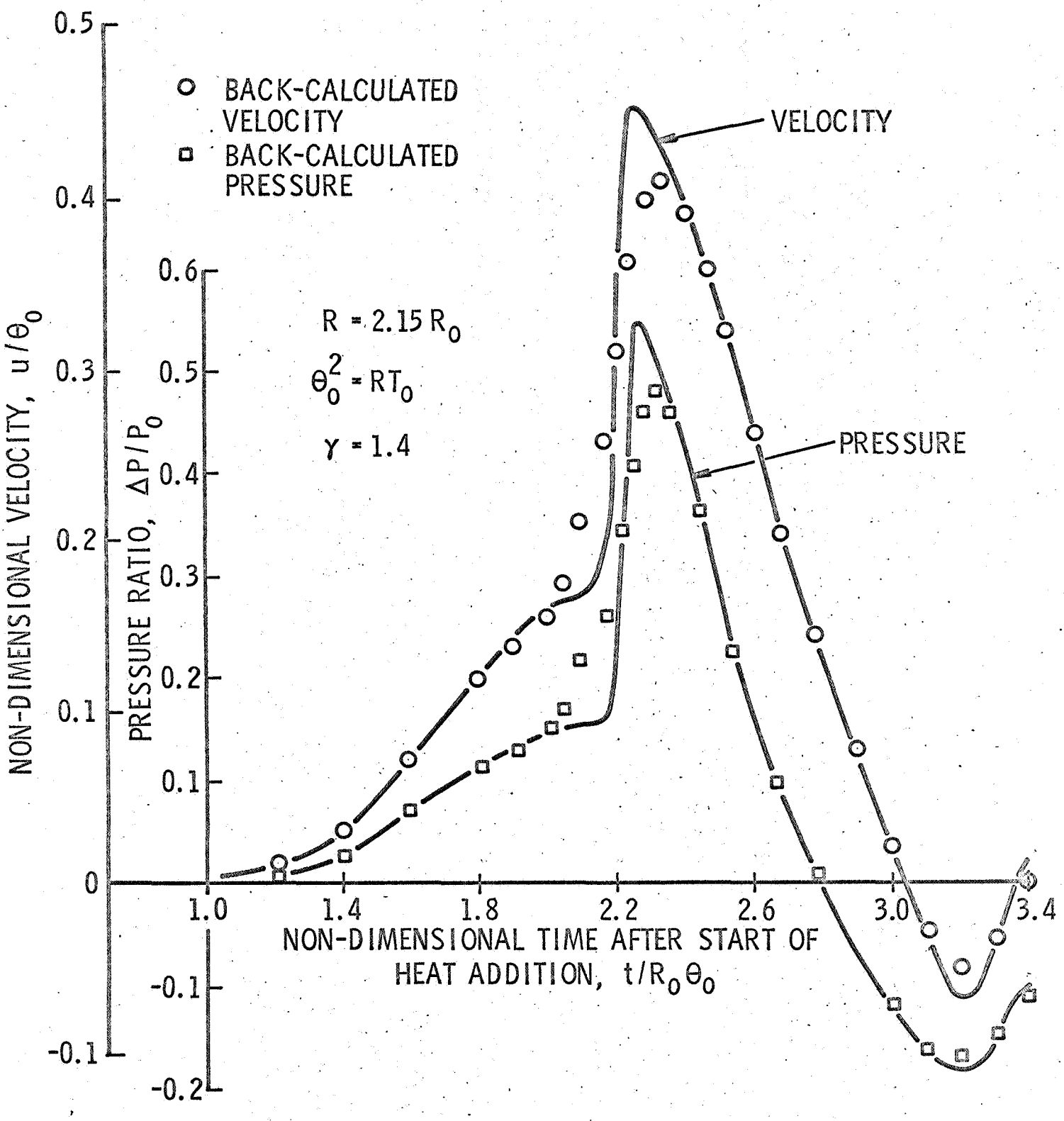

Figure 6. Comparison of "Exact" Flow Variables with Calculations, Sample Starting Conditions of Fig. 2 and Fig. 3.

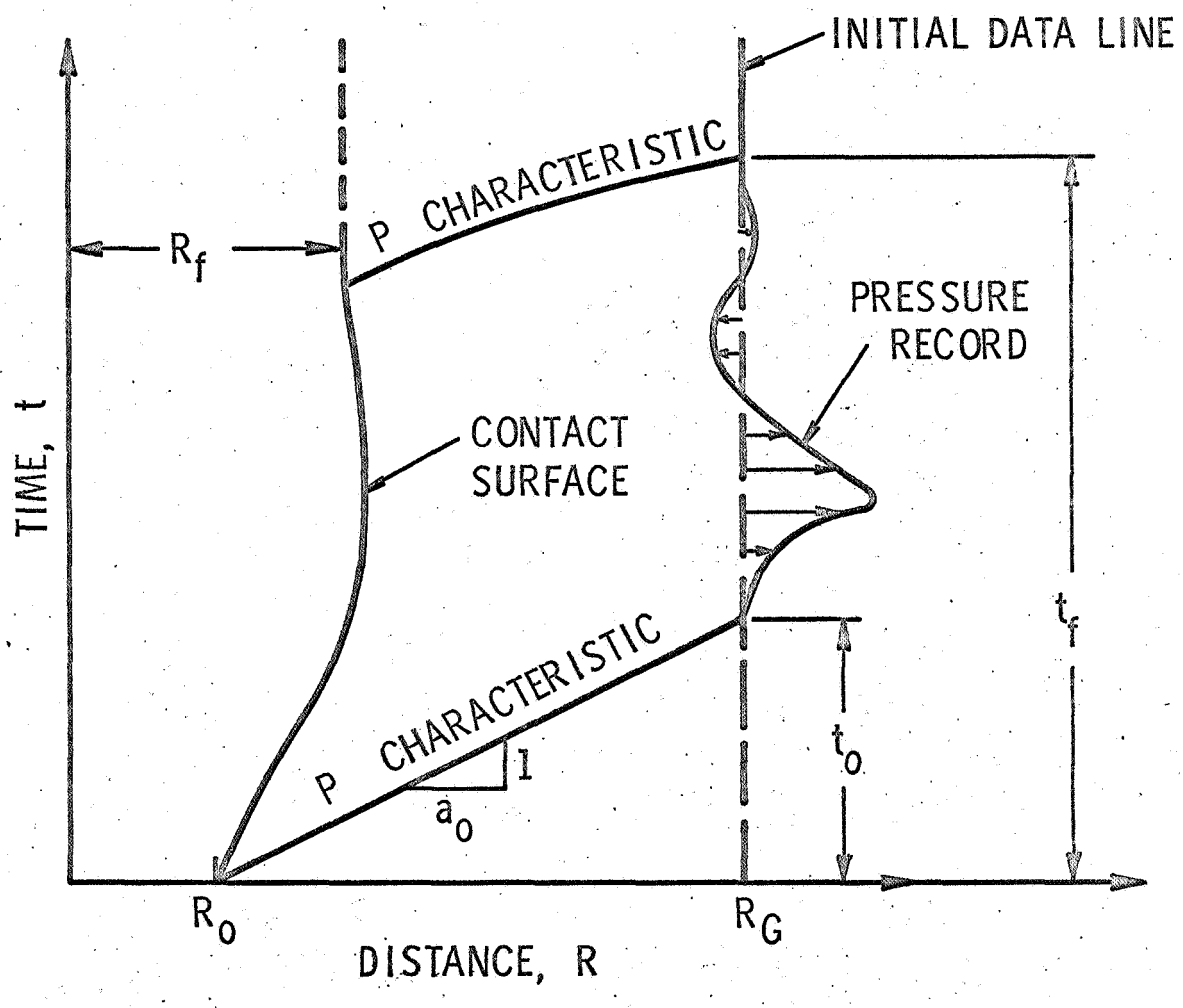

Figure 7. Expanding Cloud Model

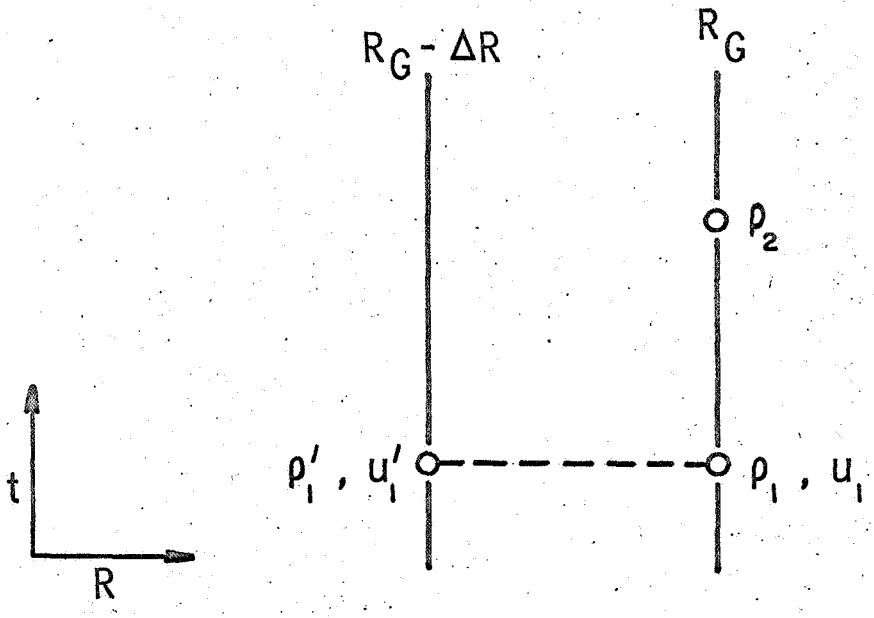

CONSERVATION OF MASS: $$\frac{\partial \rho}{\partial t} + \frac{\partial (\rho u)}{\partial R} + \frac{2 \rho u}{R} = 0$$

FINITE-DIFFERENCE FORM: $$\frac{\rho_2 - \rho_1}{\Delta t} + \frac{\rho_1 u_1 - \rho_1' u_1'}{R_G - 1/2 \Delta R} + \frac{2 \rho_1 u_1}{R_G} = 0$$

Figure 8. Method for Correcting Input Data

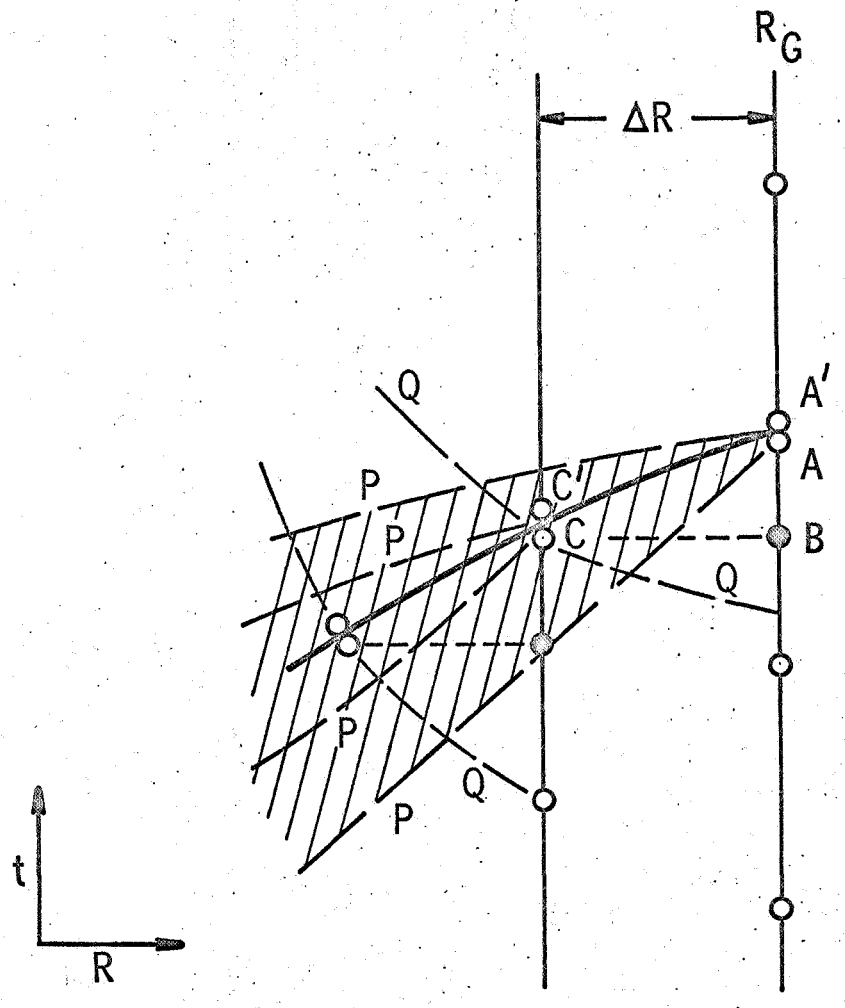

Figure 9. Method for Including Shock Waves

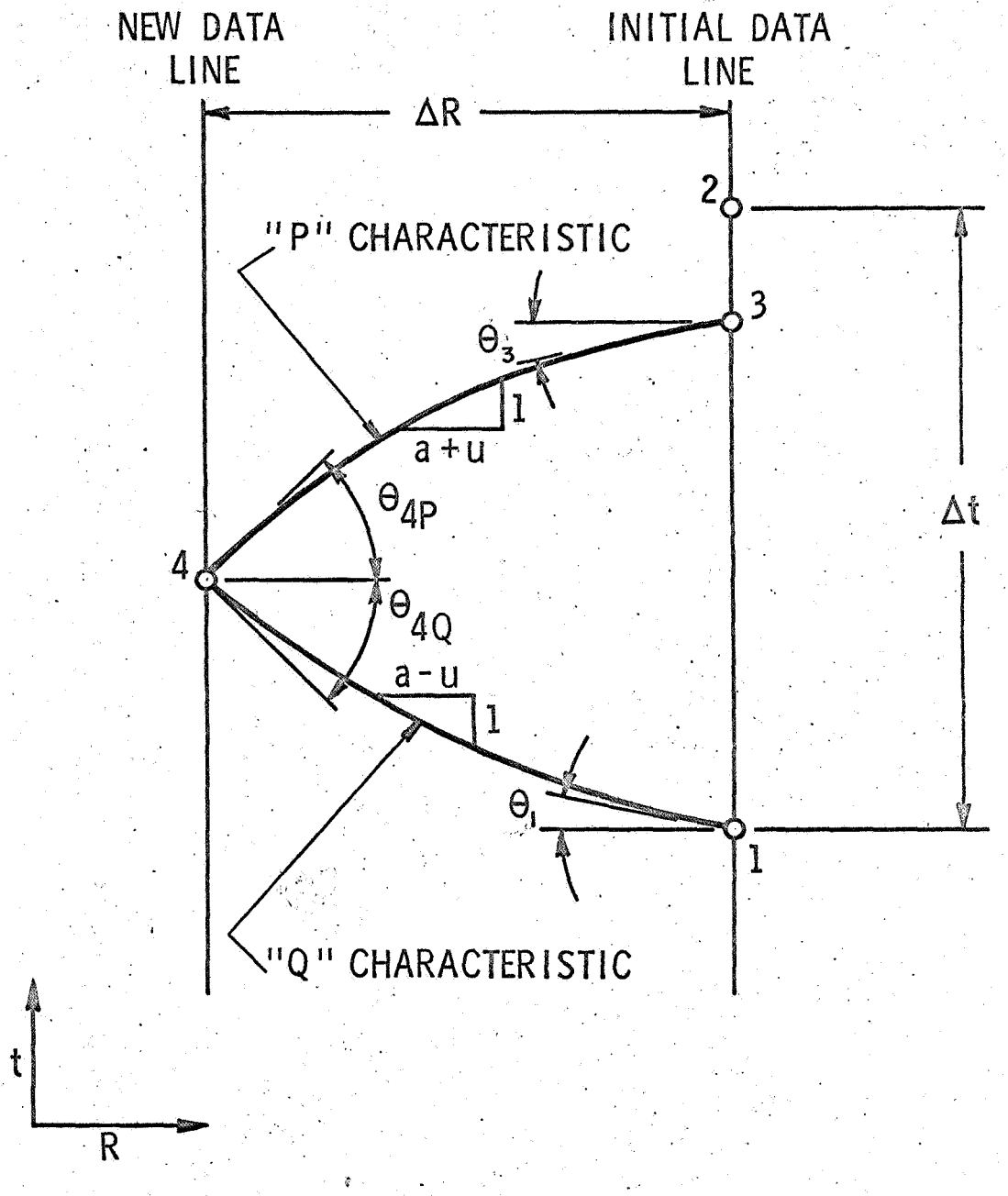

Figure A.1 Calculation of New Data Point